remote sensing

Article

A Very High-Resolution Urban Green Space from the Fusion of Microsatellite, SAR, and MSI Images

Fatwa Ramdani

Graduate School of Humanities and Social Sciences, University of Tsukuba, Tsukuba 305-8577, Japan; fatwa.ramdani.gw@u.tsukuba.ac.jp

Abstract: Jakarta holds the distinction of being the largest capital city among ASEAN countries and ranks as the second-largest metropolitan area in the world, following Tokyo. Despite numerous studies examining the diverse urban land use and land cover patterns within the city, the recent state of urban green spaces has not been adequately assessed and mapped precisely. Most previous studies have primarily focused on urban built-up areas and manmade structures. In this research, the first-ever detailed map of Jakarta's urban green spaces as of 2023 was generated, with a resolution of three meters. This study employed a combination of supervised classification and evaluated two machine learning algorithms to achieve the highest accuracy possible. To achieve this, various satellite images were utilized, including VV and VH polarizations from Sentinel-1, multiple bands from Sentinel-2, and eight bands from Planet. The Planet data were subsequently transformed into the Red-Edge Triangulated Vegetation Index and Red-Edge Triangulated Wetness Index. The data training and testing samples for urban green spaces were obtained using the Street View images available on Google Maps. The results revealed that using the Random Forest classifier algorithm and only eight bands of Planet images achieved an accuracy rate of 84.9%, while a combination of multiple images achieved an impressive 95.9% accuracy rate. Jakarta's urban areas cover approximately 33.2% of green spaces. This study provides unprecedented insights into the type, size, and spatial distribution of Jakarta's urban green spaces, enabling urban residents and stakeholders to explore and promote healthier living and better manage these green areas. Additionally, a previously unexplored concept, Jakarta's urban green belt, is introduced.

Keywords: urban green space; Jakarta; Sentinel-1; Sentinel-2; Planet; Red-Edge Triangulated Index

check for updates

Citation: Ramdani, F. A Very High-Resolution Urban Green Space from the Fusion of Microsatellite, SAR, and MSI Images. *Remote Sens.* **2024**, *16*, 1366. https://doi.org/10.3390/rs16081366

Academic Editor: Weiqi Zhou

Received: 4 March 2024
Revised: 10 April 2024
Accepted: 10 April 2024
Published: 12 April 2024

1. Introduction

Urban green space (UGS) provides the residents of a city with various benefits, including improved public health and well-being [1–3], social sustainability [4], contact with nature [5], and ecosystem service [6]. Some studies have argued that UGS also provides benefits to older people [7,8] and improves mental health [9,10].

Studies have defined UGS through greenness. Greenness can be quantified using spectral indices like the Normalized Vegetation Difference Index (NDVI) [11]. Another study classified UGS from a combination of hyperspectral images and LiDAR data [12]. Both studies utilized spectral-based analysis to classify UGS using Earth observation data. A recent study [13] presented a method for classifying UGS based on their features using a deep learning approach. However, this method requires significant computational resources due to its complexity.

A comprehensive study was conducted to evaluate the usage of UGS on a national scale, utilizing big data analysis. It also considered the variations in UGS utilization between areas within the city (intra-urban) and its outskirts (peri-urban). The study encompassed 366 cities across mainland China. The results indicated that 94.01% of UGS in China remained unused. This study used data with a spatial resolution of 1 km × 1 km [14]. Another study conducted in Xiamen, China, aimed to assess the fairness of UGS and explored how they are distributed in relation to urbanization. The study discovered that increased urbanization correlated with a greater provision of UGS services. It used images of Landsat-8 OLI from 2015 with a spatial resolution of 30 m $\times$ 30 m [15]. A study conducted in 2017 across 371 major cities in Latin America resulted in the creation of the first 10 m resolution UGS map for the main urban clusters. This study utilized a supervised classification method on Sentinel-2 satellite images and achieved an accuracy rate of 87% [16].

The increasing collection of remote sensing images from MODIS, Landsat, and Sentinel series, along with the availability of cloud-based image processing platforms such as Google Earth Engine (GEE), have the potential to enhance the UGS classification maps. However, the public currently has access to a maximum spatial resolution of 10 m. In this study, the use of Planet datasets was introduced, which offer a higher spatial resolution of 3 m.

The current methods and technologies used to monitor urban green spaces, such as aerial photography and satellite imagery, have some limitations. Aerial photogrammetry can provide very high spatial resolution but only covers small areas. To cover larger areas, more time and expense are required. Meanwhile, satellite imagery offers broader coverage but suffers from low spatial resolution. Another challenge arises from cloud coverage in tropical countries like Indonesia.

To address these issues, the suggestion in this study is to utilize Sentinel-1 SAR data to overcome cloud cover challenges. Additionally, there are existing gaps or limitations in current research concerning urban green space monitoring. For instance, accurately mapping and quantifying green spaces in densely built urban environments, such as Jakarta, poses significant challenges. Moreover, there is insufficient integration of multiple remote sensing data sources for comprehensive analysis.

Thus, in this study, the proposal is to integrate multiple remote sensing data sources, including microsatellite, SAR, and MSI, to potentially benefit from improved accuracy, enhanced feature detection, and better discrimination of urban green space types.

Integrating satellite data from different sensors is a common approach in remote sensing. To the best of the author's knowledge, two studies have partially quantified the improvement from applying a machine learning approach to Planet data within GEE. A previous study integrated Planet imagery with Sentinel-1 and Sentinel-2 data to create land use and land cover maps for Central Brazil. It compared pixel- and object-based methods using solely Planet data, as well as a combination of Planet, Sentinel-1, and Sentinel-2 data. The findings revealed that utilizing this combined dataset enhanced classification accuracy [17]. Another study combined Planet imagery, Landsat-8, and Sentinel-2 to classify land use land cover maps of Central Italy using GEE [18]. In this study, the comparison was made between pixel- and object-based approaches using the Random Forest (RF) and Support Vector Machine (SVM) algorithms. The results revealed that the RF algorithm achieved greater accuracy than SVM when classifying land use and land cover. Additionally, it was noted that the object-based method can be resource-intensive, particularly when dealing with higher-resolution data, given the computational constraints of Google Earth Engine (GEE).

The objective of this study is to produce a very high-spatial-resolution UGS map for Jakarta city with over 10 million urban inhabitants [19]. Two machine learning algorithm classifiers, namely Random Forest (RF) and Classification and Regression Tree (CART), will undergo evaluation. This study aims to assess the pixel-based classification results by utilizing solely Planet data and a combination of Planet, Sentinel-1, and Sentinel-2 data through a supervised approach.

2. Methodology

2.1. Study Area

This study is focused on Jakarta, the capital city of Indonesia (Figure 1). Jakarta covers an area of 661.23 km^2 and is located in the western part of Java Island. It is divided into five administrative areas: North Jakarta (147.46 km^2), West Jakarta (125 km^2), Central Jakarta (47.56 km^2), East Jakarta (185.54 km^2), and South Jakarta (144.94 km^2) [20].

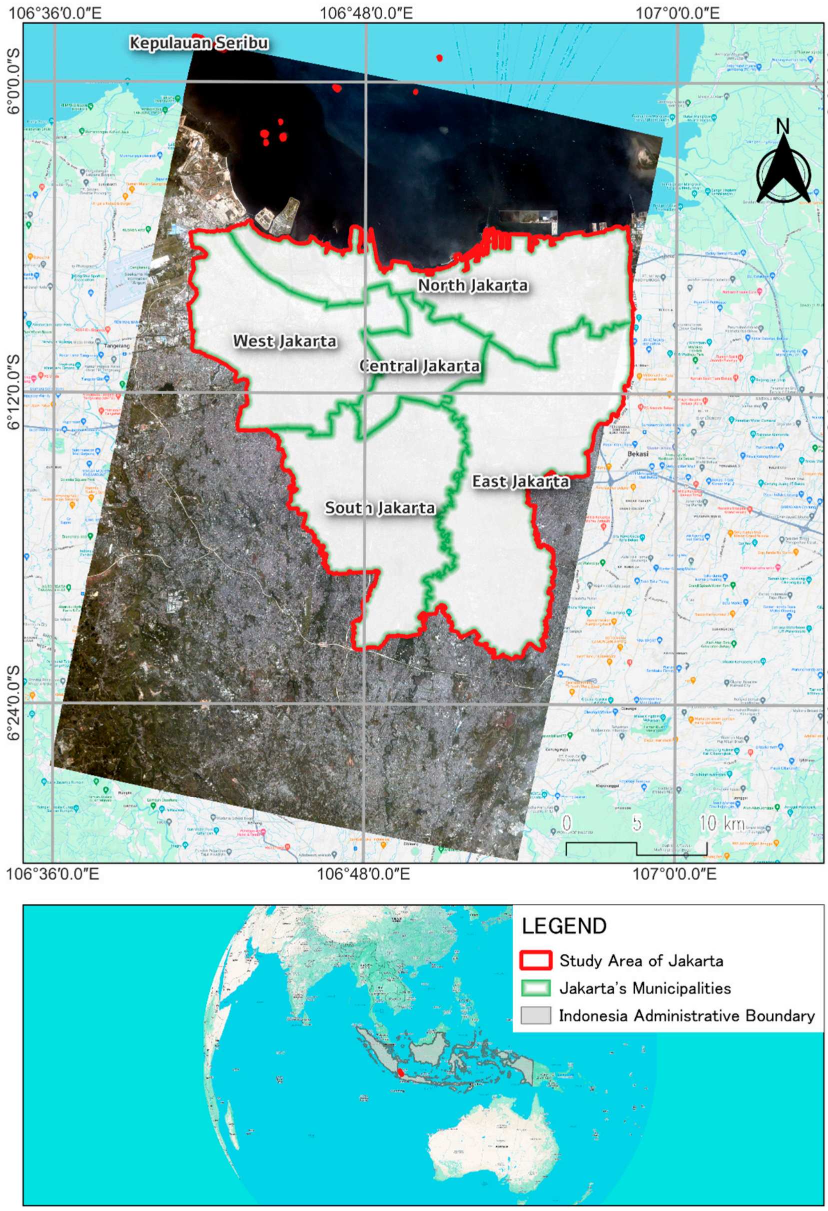

Figure 1. Jakarta as the study area overlaid with the Planet dataset. The base map is Google Road. QGIS version 3.22.8-Białowieża was used to create the map.

Despite being the smallest province in Indonesia in terms of land area, in terms of population, Jakarta boasts the largest metropolitan area in the ASEAN and the second-largest in the world, surpassed only by Tokyo, Japan [21]. Jakarta is characterized by its extensive urban development and numerous manmade structures, making it the most densely populated city in Indonesia. This high population density is one of the key reasons for selecting Jakarta as the study area. Additionally, the city was chosen due to its diverse urban green spaces and the most updated availability of ground truth samples from Google Maps Street View images.

2.2. Satellite Datasets: PlanetScope, Sentinel-1, and Sentinel-2

The PlanetScope satellite constellation comprises approximately 130 microsatellites, also referred to as CubeSats. These CubeSats have dimensions of 10 cm × 10 cm × 30 cm, with a daily temporal resolution, three-meter spatial resolution, 12-bit radiometric resolution, and eight spectral bands [22].

The initial PlanetScope satellites were launched in 2018, featuring only four spectral resolutions. The second generation is known as PS2.SuperDove (PS2.SD) or Dove-R, which became available from 2019 to 2022. The third generation is also referred to as SuperDove or PSB.SD, now boasts eight spectral bands, namely coastal blue (b1), blue (b2), green I (b3), green (b4), red (b5), yellow (b6), red edge (b7), and near-infrared (b8).

In this study, the PlanetScope data were obtained through an education and research standards license. These data were captured on 14 August 2023, encompassing three scenes that encompassed the study area. These scenes provide surface reflectance products at the analytic level, comprising eight bands. The data were accessed from https://www.planet.com/explorer/ (accessed on 12 December 2023) and imported into QGIS software version 3.22.8-Białowieża, and they were subsequently merged. The resulting merged dataset was then uploaded to the Google Earth Engine (GEE) platform as an asset for additional processing. In the GEE platform, the PlanetScope data were transformed into the Red-Edge Triangulated Vegetation Index (RTVI) and the Red-Edge Triangulated Wetness Index (RTWI) spectral indices using the first and second equations, respectively, as follows:

$$RTVI = (100 * (NIR - RedEdge) - 10 * (NIR - Green)) \quad (1)$$

$$RTWI = (100 * (RedEdge - NIR) - 10 * (Green - Red)) \quad (2)$$

The RTVI and RTWI were chosen to monitor the red-edge band, which is known to be responsive to subtle variations in vegetation health. This choice enables a unique method to address situations where the Normalized Difference Vegetation Index (NDVI) becomes saturated in regions with extensive, dense vegetation or crops, limiting its effectiveness in capturing changes [23].

Sentinel-1 is a part of the European Space Agency (ESA) and consists of two constellations: Sentinel-1A and Sentinel-1B. This system is equipped with an active remote sensing sensor that gathers data using dual-polarization C-band Synthetic Aperture Radar (SAR). Its spatial resolution is 10, 25, and 40 m, and it captures data every 6 to 12 days [24].

In this study, the Sentinel-1 data in vertical–vertical (VV) and vertical–horizontal (VH) polarizations were used, which were acquired in interferometric wide (IW) swath mode, with ascending properties, during the post-rainy season (April to September 2023). This ensured comprehensive coverage of the study area.

The queried Sentinel-1 data were processed to calculate the inter-quartile range (IQR) as a measure of backscatter variability. All of the Sentinel-1 data used in this study were ground-range-detected (GRD) and readily available in the Google Earth Engine (GEE) data catalog.

Sentinel-2, like Sentinel-1, is part of the ESA program and consists of two satellite constellations: Sentinel-2A and Sentinel-2B. However, unlike Sentinel-1, Sentinel-2 employs a passive remote sensing sensor equipped with a multispectral imaging (MSI) sensor capable of capturing data in 13 spectral bands. It offers variable spatial resolutions of 10, 20, and 60 m and a temporal resolution of 10 days at the equator with one satellite, and 5 days with two satellites under cloud-free conditions [25].

For this study, Sentinel-2 MSI Level-2A datasets available in the Google Earth Engine (GEE) data catalog were utilized. All bands were incorporated into the classification process, except for bands 1 and 9, which are primarily sensitive to aerosols and water vapor, respectively, and have a lower spatial resolution of 60 m.

In line with Sentinel-1, the acquisition period for Sentinel-2 was also after the rainy season, spanning from April to September 2023. The queried data underwent preprocessing to remove cloud cover from the scenes. Only scenes with clear conditions proceeded to the next stages of processing.

2.3. Training and Validation Datasets

Based on the understanding of the study area, several polygons were manually generated using the GEE platform. Street View images from Google Maps were used as a reference to ensure accuracy and verify the latest conditions. As depicted in Figure 2, paddy fields were observed in North Jakarta as of July 2023.

Figure 2. A street view image of a specific area in the part of the study area (North Jakarta) was utilized as a point of reference to ensure precision and verify its current condition. Source: Google Street View (https://shorturl.at/nsFWX, (accessed on 12 July 2023)).

In total, over 100 polygons were created randomly and categorized into six distinct classes of urban green spaces: agriculture, forest, grassland, mixed, shrub, and wetland. Further details regarding these categories are presented in Table 1.

Table 1. Urban green space categories.

Categories	Description
Agriculture	Paddy field, farm or farmland, orchard, plant nursery
Forest	Forest, nature reserve, big tree
Grassland	Grass, meadow, golf, sports center, grassland, football fields, baseball fields, airport fields
Mixed	Recreation ground, residential green, riparian zone, disc golf course, garden, park, campsite, cemeteries
Shrub	Small trees, persistent woody stems above the ground
Wetland	Wetland, mangroves

Furthermore, the Pareto Principle was applied to split the created multiple polygons into 70% for training data and 30% for testing data.

2.4. Machine Learning Algorithms and Classification

Two machine learning algorithms were assessed: Random Forest (RF) and Classification and Regression Tree (CART). These algorithms were chosen because they all rely on decision trees and can be compared. RF is an ensemble learning technique based on decision trees [26], suitable for categorical data, unbalanced data, and data with missing values [27], and it is renowned for its high accuracy and robustness in handling remote sensing data [28]. The CART classifier algorithm is a commonly used tree-based framework in remote sensing applications [29]. It starts by examining all input variables and identifying the optimal binary split of a single variable that minimizes the deviation in the output variable. In the case of the classification of Earth observation data, the input variables include spectral and additional data, whether they are continuous or categorical, and the output variable is the list of land use and land cover classes [30]. The crucial step in determining the structure of a decision tree is choosing an input feature and a threshold value for each split [31].

Before initiating the classification process, it is imperative to consolidate all datasets. To elaborate, this consolidation encompassed two polarization channels from Sentinel-1; nine spectral bands from Sentinel-2; eight bands from PlanetScope; and two specific indices, namely RTVI and RTWI. Subsequently, the training dataset was employed to train the classifier algorithms, culminating in the execution of the classification process.

The unit analysis for classification involved the use of administrative boundaries. These administrative boundaries were derived from the Global Administrative Unit Layers (GAUL) Level-2 dataset [32], which is accessible through the GEE data catalog. There are a total of five administrative boundaries, namely North Jakarta, West Jakarta, Central Jakarta, East Jakarta, and South Jakarta. The classification results were subsequently clipped based on these administrative boundaries.

2.5. Accuracy Assessment, Data Conversion, and Area Calculation

The classification results were subsequently assessed using the matrix contingency method. Finally, the classified images were exported to Google Drive, downloaded, and imported into the QGIS environment for the final visualization process.

In the QGIS environment, the raster layer was first polygonized, and its geometry was subsequently fixed. Next, a new "Class" field was created to categorize each "Digital Number (DN)" value into distinct classes using a "CASE statement" within the field calculator feature. Afterward, the vector layer was dissolved based on the "Class" field. Using the resulting dissolved vector layer, the final area of each urban green space class was calculated. Only areas larger than 0.1 km^2 were considered for analysis, while the rest were excluded. To refine the data, Google's Open Building Data accessible through the GEE data catalog was utilized. Specifically, only data with a confidence level of 75% or higher were selected. Subsequently, the "Difference" function in the "Geoprocessing Tools" of QGIS was employed. Vector data were manipulated to create a highly accurate urban green space map for Jakarta, where the "input layer" and "difference layer" are urban green space data and open building data, respectively. Figure 3 provides a summary of the methodology that was developed and employed in this study.

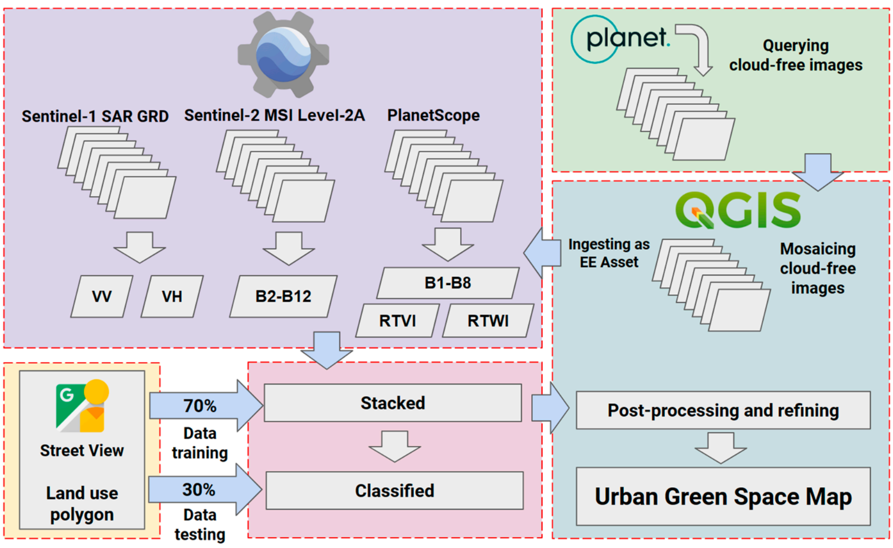

Figure 3. Methodology of the study.

3. Results

3.1. Classification Results and Model Performance

Table 2 displays the overall accuracy values for the classification obtained from two different classifier algorithms. This table provides information on the selected features (bands) and their importance variables in each classifier.

Table 2. Classifier algorithm performance.

	RF		CART	
	PlanetScope Only	**Multiple Images**	**PlanetScope Only**	**Multiple Images**
Overall accuracy (%)	84.9	95.9	85.1	87.7
Variable of importance	B2 (Blue), B8 (NIR), and B7 (Red Edge)	B7 (Red Edge 3) of Sentinel-2, B1 (Coastal Blue) of PlanetScope, and B12 (SWIR 2) of Sentinel-2	B1 (Coastal Blue), B2 (Blue), and B3 (Green)	B2 (Blue) of Sentinel-2, B1 (Coastal Blue) of PlanetScope, and B6 (Red Edge 2) of Sentinel-2

When utilizing only the PlanetScope dataset and the RF classifier algorithm, a good accuracy of 84.9% was achieved. However, when combining multiple images, the accuracy increased significantly to 95.9%. In the case of CART classifier algorithms, using only the PlanetScope dataset yielded an 85.1% accuracy, which increased slightly to 87.7% when multiple images were employed.

When employing the RF classifier algorithm and a single PlanetScope dataset, the most crucial values were derived from B8 (NIR), B2 (Blue), and B7 (Red Edge). When using multiple images, the most crucial values were derived from band RTVI, followed by band B2 (Blue) of Sentinel-2, and band B1 (Coastal Blue) of Planet. In contrast, when using the CART classifier algorithm and a single PlanetScope dataset, the most crucial values were derived from B1 (Coastal Blue), B2 (Blue), and B3 (Green). When using multiple images, the most significant values were associated with band B2 (Blue) of Sentinel-2, followed by band B1 (Coastal Blue) of PlanetScope and band RTVI.

The performance of the RF classifier algorithm showed that almost all the bands used made a significant contribution to the classification. In contrast, the CART classifier algorithm's performance indicated that only certain bands were significant contributors to the classification, while others were not. For instance, when using only PlanetScope bands, B1 (Coastal Blue) was significant, whereas the other bands were not. When utilizing multiple images, only B2 (Blue) from Sentinel-2 significantly contributed to the classification. Table 3 summarizes the details.

The differences between RF and CART in the feature importance are because of five factors: algorithm differences, randomness in RF, correlation among features, model complexity, and interpretability.

RF and CART are two different algorithms used for classification tasks. Random Forest is an ensemble learning method that builds multiple decision trees and merges their outputs to improve accuracy and generalize well on unseen data. CART, on the other hand, typically refers to a single decision tree. The differences in how these algorithms construct decision boundaries and handle feature interactions can lead to variations in feature importance.

RF introduces randomness in the feature selection process by considering a random subset of features for each split in each decision tree. This random selection process can cause different subsets of features to be chosen as important across different trees, leading to a diverse set of feature importance rankings. In contrast, CART typically considers all features for each split, potentially leading to a more consistent feature importance ranking.

Table 3. Variable of importance.

RF

PlanetScope only

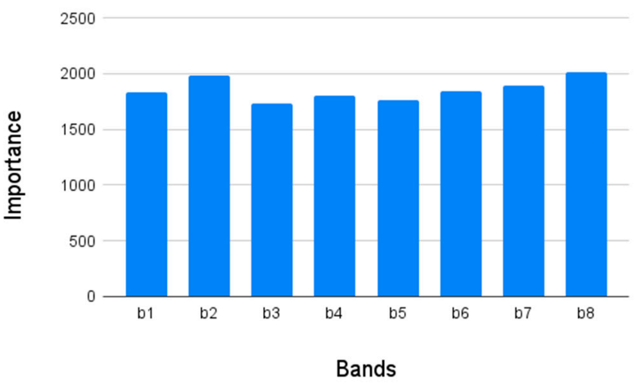

Multiple images

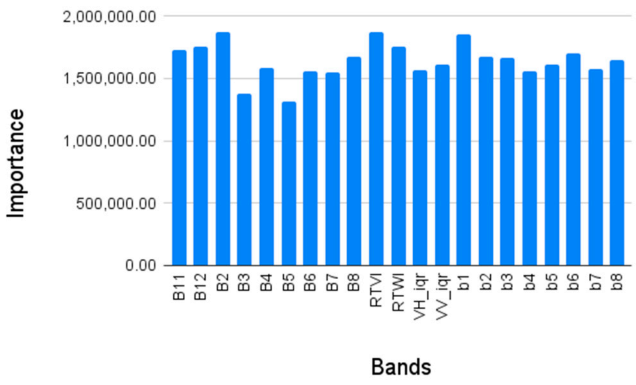

CART

PlanetScope only

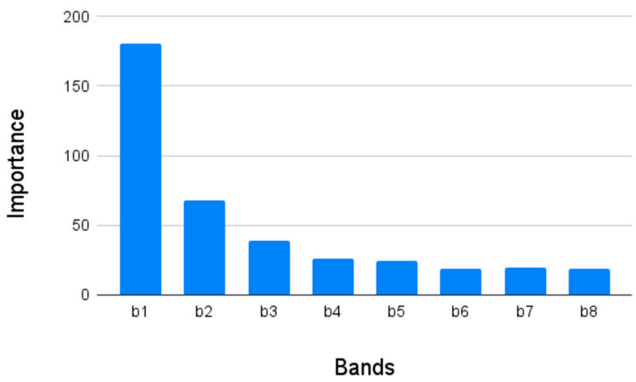

Multiple images

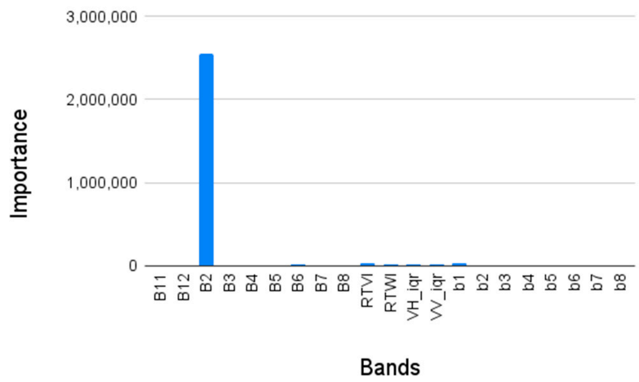

Since PlanetScope and Sentinel-2 consist of multispectral bands, each capturing different aspects of the Earth's surface, some bands may be highly correlated with each other, meaning they convey similar information. In RF, the algorithm can exploit this redundancy by randomly selecting a subset of features at each split, which may lead to different bands being considered important in different trees. CART, on the other hand, may consistently choose one of the correlated bands over others, resulting in different feature importance rankings.

Furthermore, RF tends to be more robust to overfitting compared to CART, especially when dealing with high-dimensional data like satellite images. As a result, RF may capture more complex relationships between features and the target variable, leading to different feature importance rankings compared to CART, which may prioritize simpler relationships.

CART decision trees are generally easier to interpret compared to RF, as they represent simple decision rules. The simplicity of CART models may influence the feature importance rankings, as they tend to highlight features that have a more direct impact on the classification decision.

Table 4 presents a cartographic comparison of two classification results for the study area, which were obtained using the two different classifier algorithms. The colors on the map correspond to six distinct categories of urban green spaces (lavender pink for agriculture, dark green for forest, yellow for grass, gold for mixed, deep saffron for shrubs, and pacific blue for wetland), while red indicates urban built-up areas with manmade structures and blue signifies water bodies, such as coastlines, lakes, rivers, or reservoirs.

Table 4. Classification results.

RF	
PlanetScope only	Multiple images
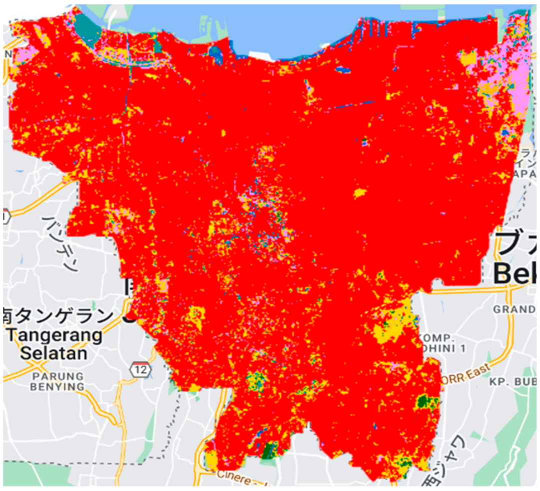	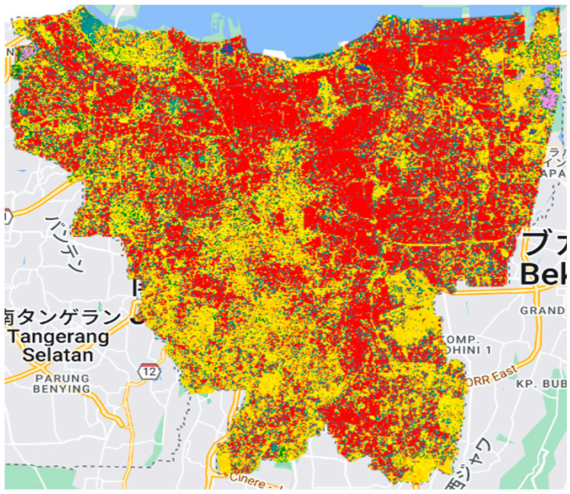
CART	
PlanetScope only	Multiple images
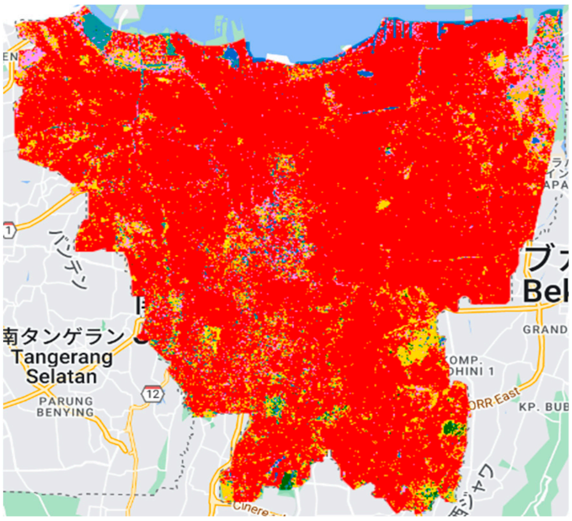	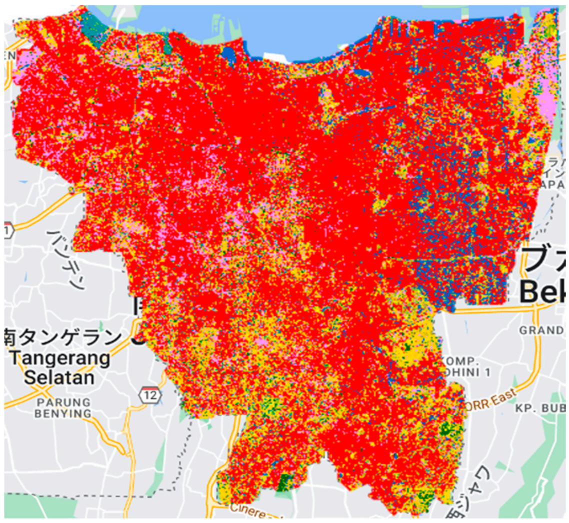

When using only PlanetScope bands, it becomes evident that the classification is heavily skewed toward urban built-up areas and manmade structures, resulting in a reduced accuracy in classifying urban green spaces. However, the inclusion of multiple bands from Sentinel-1, Sentinel-2, RTVI, and RTWI significantly enhanced the classification results. Both the classification maps generated by the RF classifier algorithm and the utilization of multiple images corroborated the superior performance of the classification outcomes.

3.2. North Jakarta

North Jakarta boasts the most diverse urban green spaces compared to other administrative regions. It encompasses all six categories of urban green space, ranging from agriculture to wetland areas, with a total urban green space area of 51.01 km^2. Out of a total area of 147.46 km^2, 34.59% is classified as urban green spaces. The largest portion of urban green space consists of mixed areas (17.83 km^2), followed by shrubland (12.41 km^2), grassland (11.7 km^2), forested areas (3.89 km^2), wetlands (3.23 km^2), and agricultural zones (1.95 km^2) (Figure 4). Located in the northern part of Jakarta, the wetland areas are predominantly covered by mangroves (Figure 5), while the agricultural zones are mainly dominated by paddy fields.

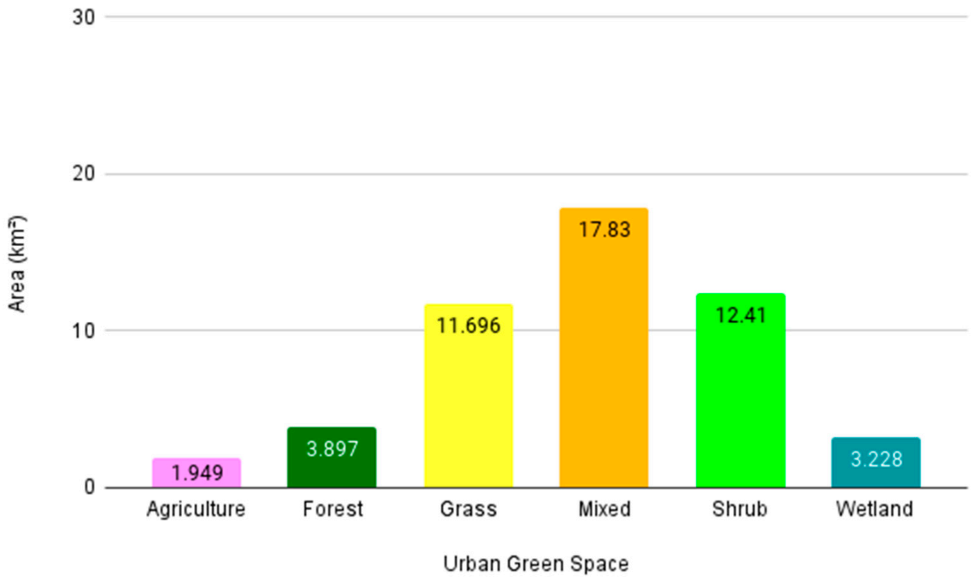

Figure 4. The portion of urban green space in North Jakarta.

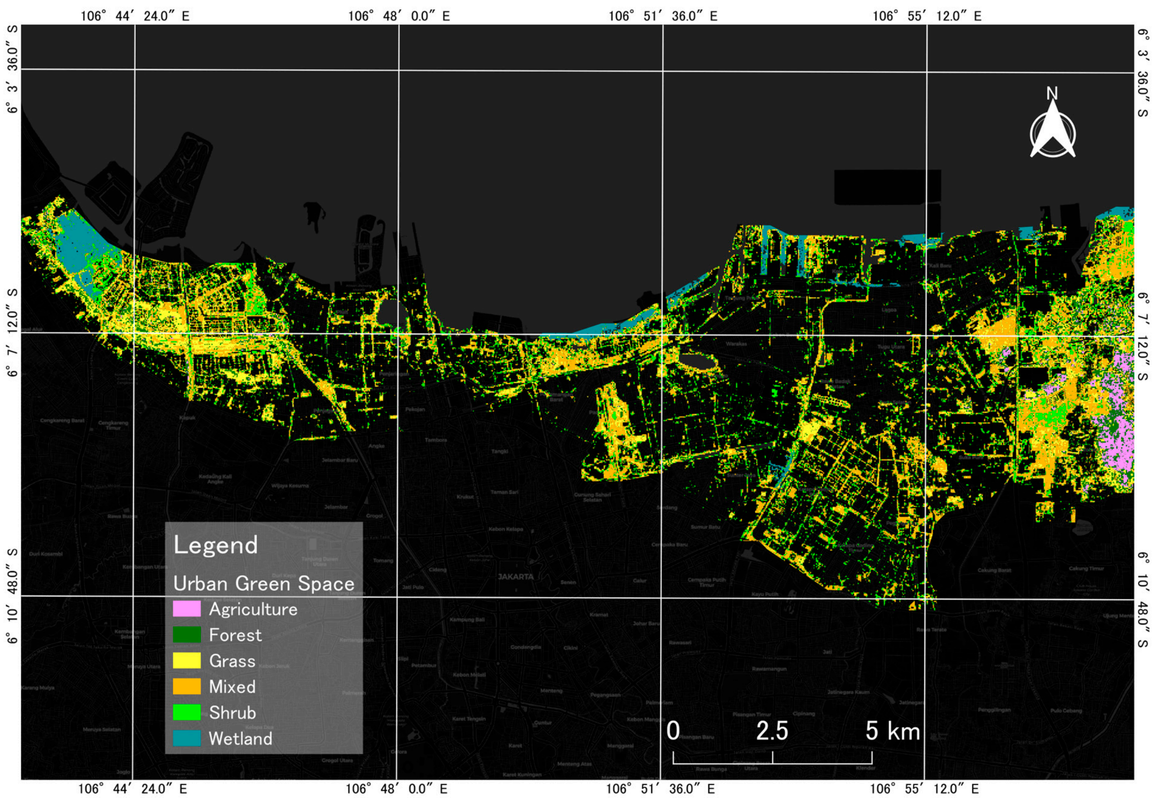

Figure 5. Urban green space of North Jakarta. The base map is CartoDB Dark Matter. QGIS version 3.22.8-Białowieża was used to create the map.

This area, formerly utilized by numerous illegal fish farmers, commenced its restoration efforts in 1998. Transforming the region from a forested area into a fishpond not only led to the removal of trees but also inflicted harm on the environment and the mangrove ecosystem. Presently, it thrives as a wetland ecosystem primarily characterized by mangrove trees. This conservation site is known as the Angke Kapok Nature Tourism Park, and it is accessible to the public.

Unfortunately, certain sections of North Jakarta's mixed urban green space are situated within the exclusive Pantai Indah Kapuk district, which is restricted to residents only. In North Jakarta, there are approximately 145 small parks accessible to the public, including a city park of Taman Hutan Kota Kebon Pisang Penjaringan, interactive parks, environmental parks, and a public building park of Taman Jakarta Islamic Center. The rest of the urban green space is green lane roads and water banks, and eleven locations provide open spaces for cemeteries.

3.3. West Jakarta

The urban green space percentage of West Jakarta is around 30.47% (38.1 km^2). The largest urban green space is grass (12.43 km^2), followed by mixed areas (10.28 km^2), shrub (8.33 km^2), and forest (6.22 km^2) (Figure 6). A small part of the urban green space of West Jakarta is agriculture, and it consists of paddy fields (Figure 7).

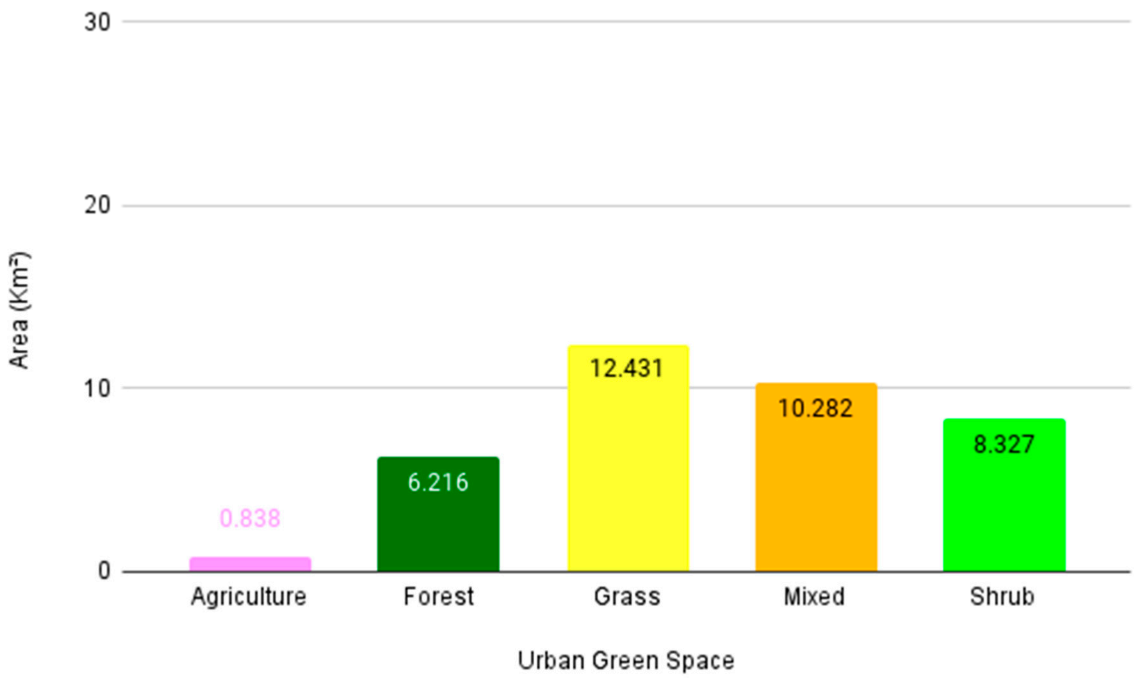

Figure 6. The portion of urban green space in West Jakarta.

In West Jakarta, there are approximately 202 small parks accessible to the public, including the city parks of Taman Hutan Kota Kampung Sawah, interactive parks, environmental parks, and a recreational park of Taman Kebun Bibit Srengseng. The rest of the urban green space is green lane roads and water banks, and there are twelve open spaces dedicated to cemeteries.

One of West Jakarta's most renowned parks open to the public is Taman Cattleya. Besides offering a place for relaxation and exercise, this park also provides an opportunity for visitors to expand their knowledge by exploring its diverse range of plant species.

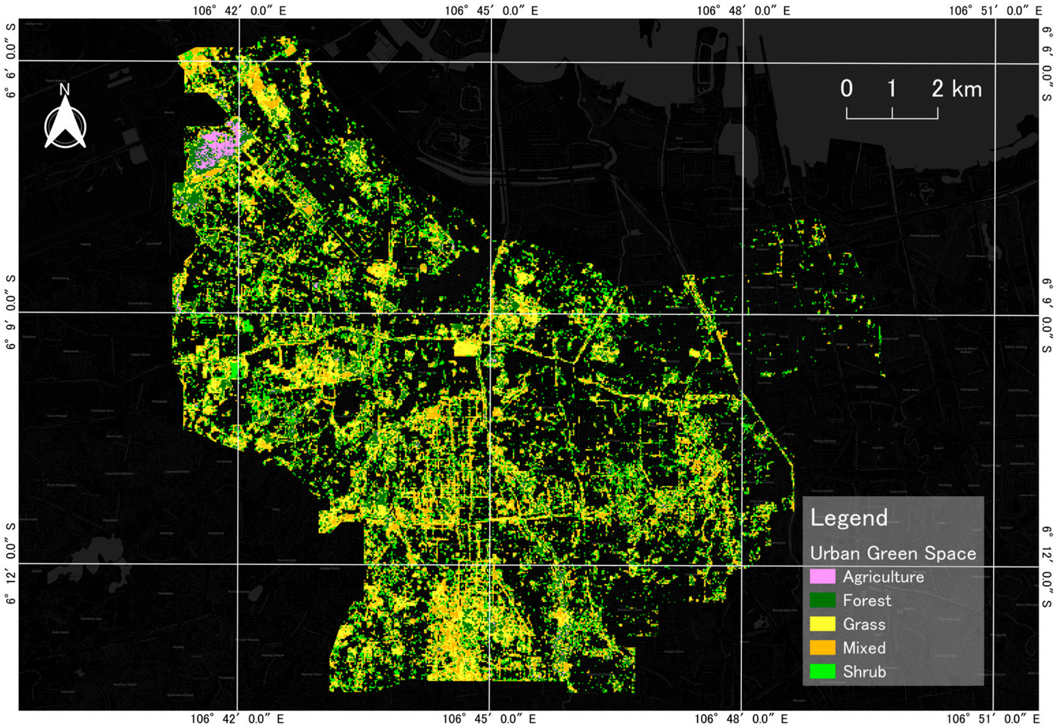

Figure 7. Urban green space of West Jakarta. The base map is CartoDB Dark Matter. QGIS version 3.22.8-Białowieża was used to create the map.

3.4. Central Jakarta

The Central Jakarta region is the smallest among the five administrative regions. It covers only 47.56 km^2, and approximately 13.25 km^2 of this area, which is roughly 27.85%, is classified as urban green space (Figure 8). This urban green space consists mainly of mixed areas (Figure 9), which cover 4.93 km^2, followed by grassland spanning 3.86 km^2; shrub-covered areas of 2.98 km^2; and a small, forested area measuring 1.48 km^2.

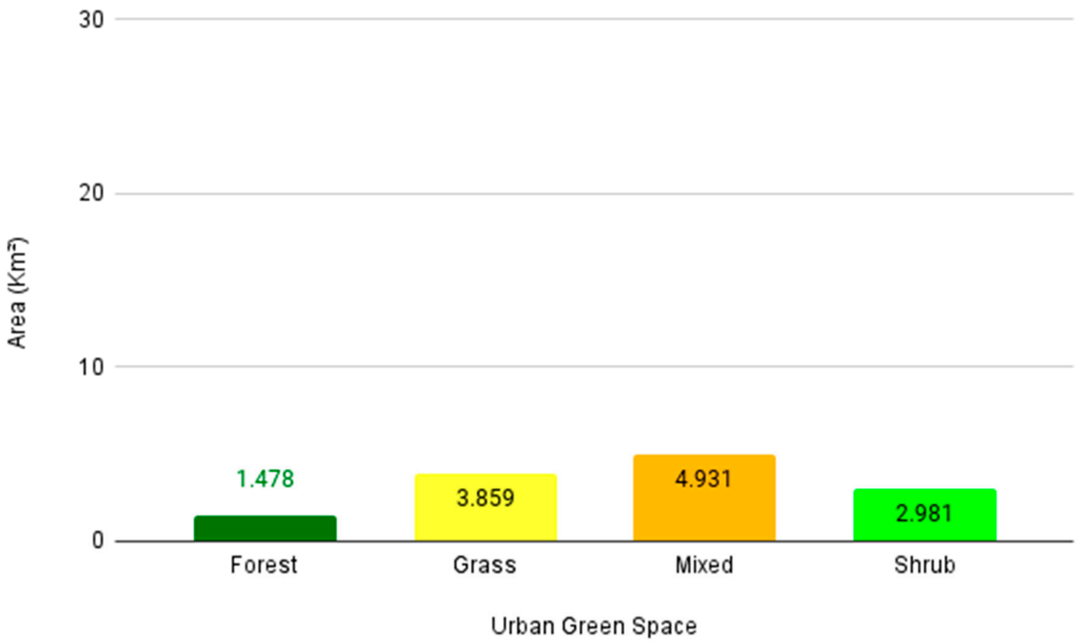

Figure 8. The portion of urban green space in Central Jakarta.

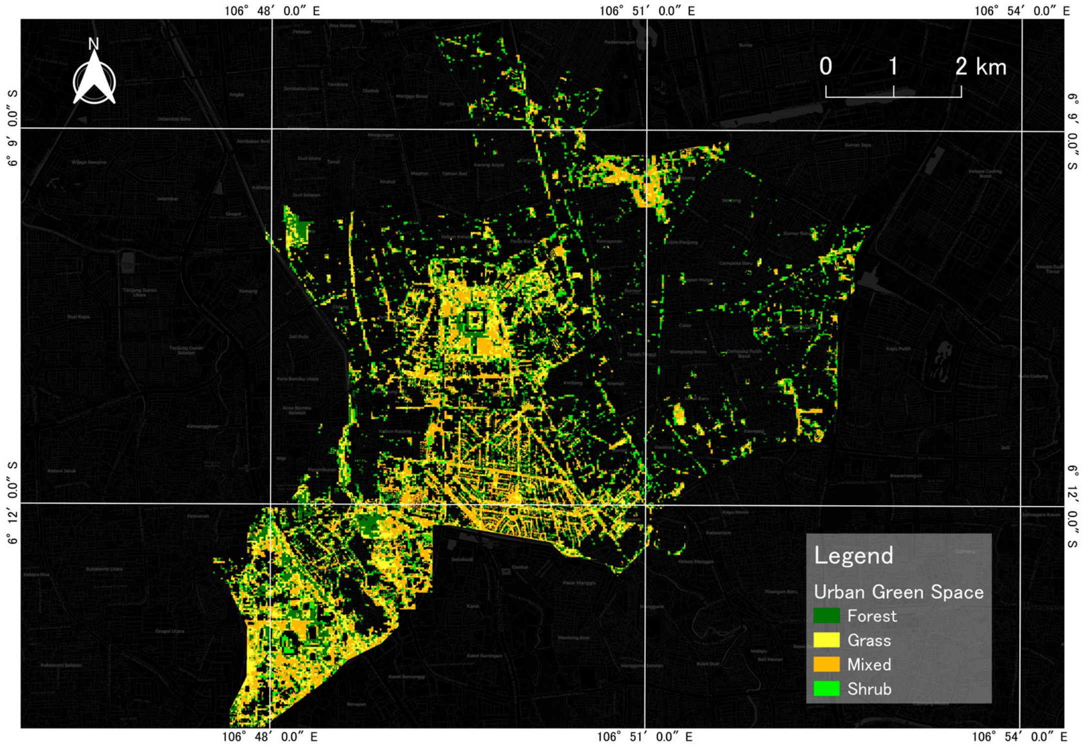

Figure 9. Urban green space of Central Jakarta. The base map is CartoDB Dark Matter. QGIS version 3.22.8-Białowieża was used to create the map.

Despite the limited availability of urban green spaces in Central Jakarta, it boasts the highest number of city parks compared to the other five administrative regions. Central Jakarta is home to five city parks, namely Taman Medan Merdeka (Monas), Taman Menteng, Taman Suropati, Taman Situlembang, and Taman Lapangan Banteng. All of these city parks are open to the public. The most famous urban green spaces that are open to public in the Central Jakarta are the Gelora Bung Karno Complex and the National Monument (Monas). Gelora Bung Karno Complex consists of multiple sports centers and city forests, while the Monas is an open green space consisting of grass, a small forest, and mixed areas.

There are 295 small interactive parks, environmental parks, and other urban green spaces, such as green lane roads and water banks. Additionally, there are four open spaces specifically designated for cemeteries.

3.5. East Jakarta

The East Jakarta region is the largest administrative area when compared to the other five regions. With a total area of 185.54 km^2, it comprises 58.27 km^2 of urban green space, which accounts for approximately 31.41% of the total area (Figure 10). This urban green space is primarily composed of mixed areas (29.4 km^2), followed by shrub-covered areas (15.64 km^2) in the second place, grass areas (11.46 km^2) in the third place, and a small portion of forest (1.51 km^2) and wetland (0.25 km^2) (Figure 11).

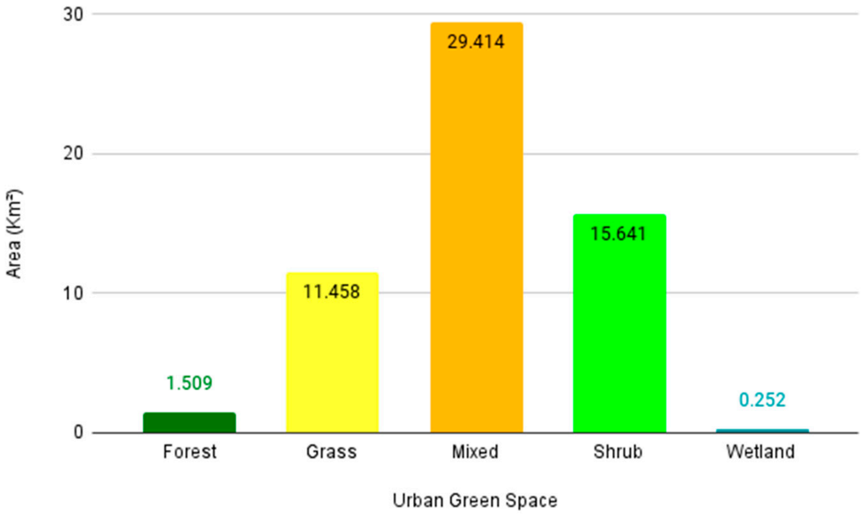

Figure 10. The portion of urban green space in East Jakarta.

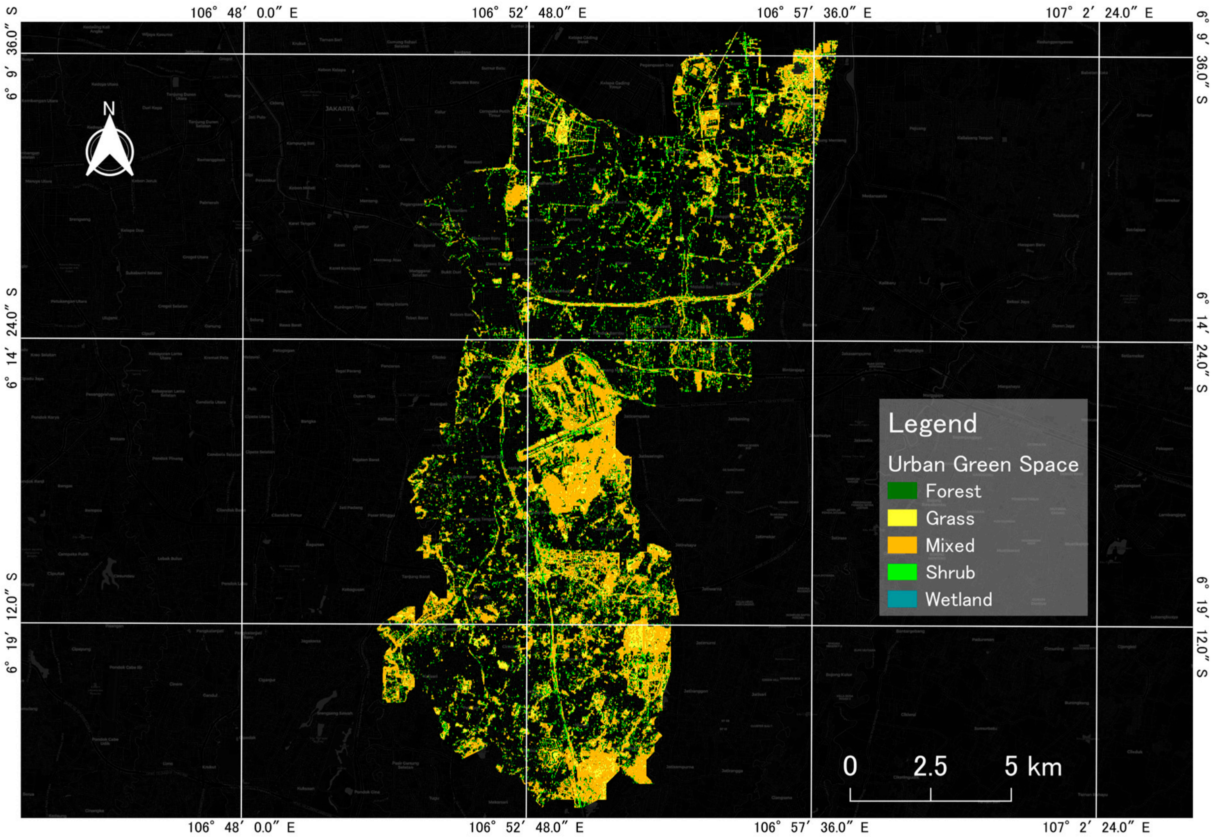

Figure 11. Urban green space of East Jakarta. The base map is CartoDB Dark Matter. QGIS version 3.22.8-Białowieża was used to create the map.

Despite being the largest area, the East Jakarta region has no dedicated city parks. Instead, it offers small interactive parks, environment parks, and a public building park. However, East Jakarta boasts the highest number of dedicated cemetery locations, totaling 28. The remaining urban green spaces serve as green lane roads and water banks.

Some parts of mixed areas in East Jakarta fall under the exclusive zone such as Royale Jakarta Golf Course, Suvarna Jakarta Golf Course, and Padang Halim Golf Course. The most famous urban green space that is open to public in the East Jakarta is the Taman Mini Indonesia Indah Complex. It offers visitors the experience of the vibrant Indonesian culture and breathtaking nature at the park, which showcases these treasures through museums, gardens, and stunning replicas of Indonesia's famous landmarks. Another urban green space is Taman Piknik, a relatively new park located in East Jakarta, which features Tabebuya trees that adorn its main area.

3.6. South Jakarta

With a total administrative area of 144.94 km^2 and 60.1 km^2 of urban green space, the South Jakarta region boasts the largest urban green space, covering approximately 54.11% of the area (Figure 12). This green space primarily comprises mixed areas (34.23 km^2), followed by shrub-covered areas (24.78 km^2), grassy expanses (16.66 km^2), and forested areas (2.76 km^2) (Figure 13).

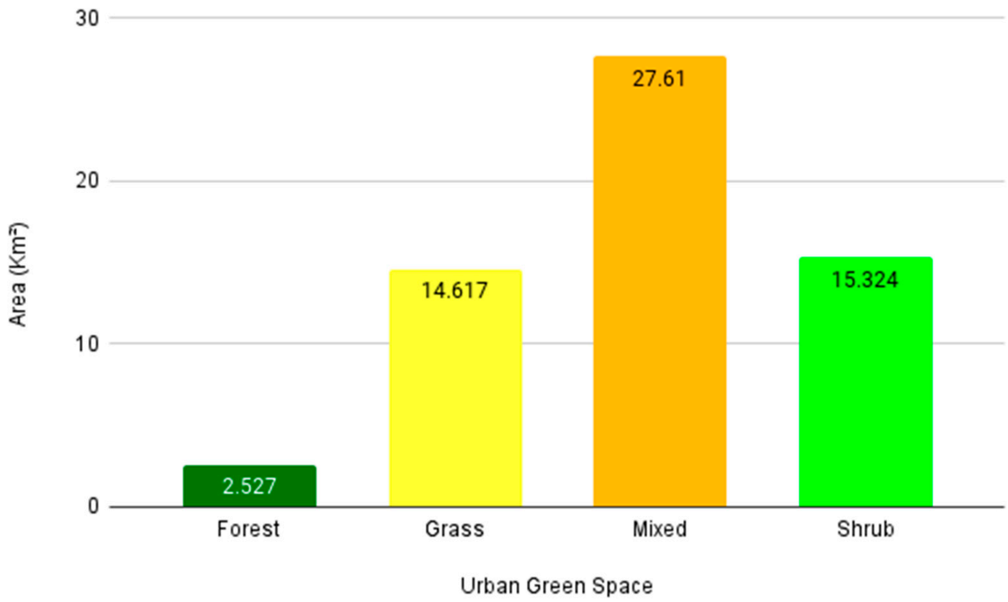

Figure 12. The portion of urban green space in South Jakarta.

In South Jakarta, there are approximately 383 small parks accessible to the public, including interactive parks, environmental parks, and public building parks. Among these, Taman Ayodia serves as a city park, while three recreational parks, namely Taman Kebun Bibit Ciganjur, Bumi Perkemahan Ragunan, and Taman Hutan Kota Tebet and Tebet Eco Park, provide additional green spaces for residents and visitors. There are a total of 18 open urban green spaces specifically designated for cemeteries in South Jakarta, while the remaining serve as green lane roads and water banks.

One of the most renowned urban green spaces open to the public in South Jakarta is Ragunan Zoo, which ranks among the five largest zoos in Indonesia. Interestingly, the zoo still features some pristine tropical rainforest within its confines, while other forests are located within the University of Indonesia's campus area in the southern part, bordering Depok City in West Java Province.

3.7. Jakarta's Urban Green Belt

Jakarta's urban green belt refers to a network of connected green spaces spanning from South Jakarta, through Central Jakarta, and up to North Jakarta. This expansive belt encompasses various types of urban green areas, ranging from agricultural zones and forests to grasslands, shrubbery, mixed-use areas, and wetlands. As depicted in Figure 14, Jakarta's urban green belt is quite extensive, covering approximately 124.34 km^2 or 19.11% of Jakarta's total land area.

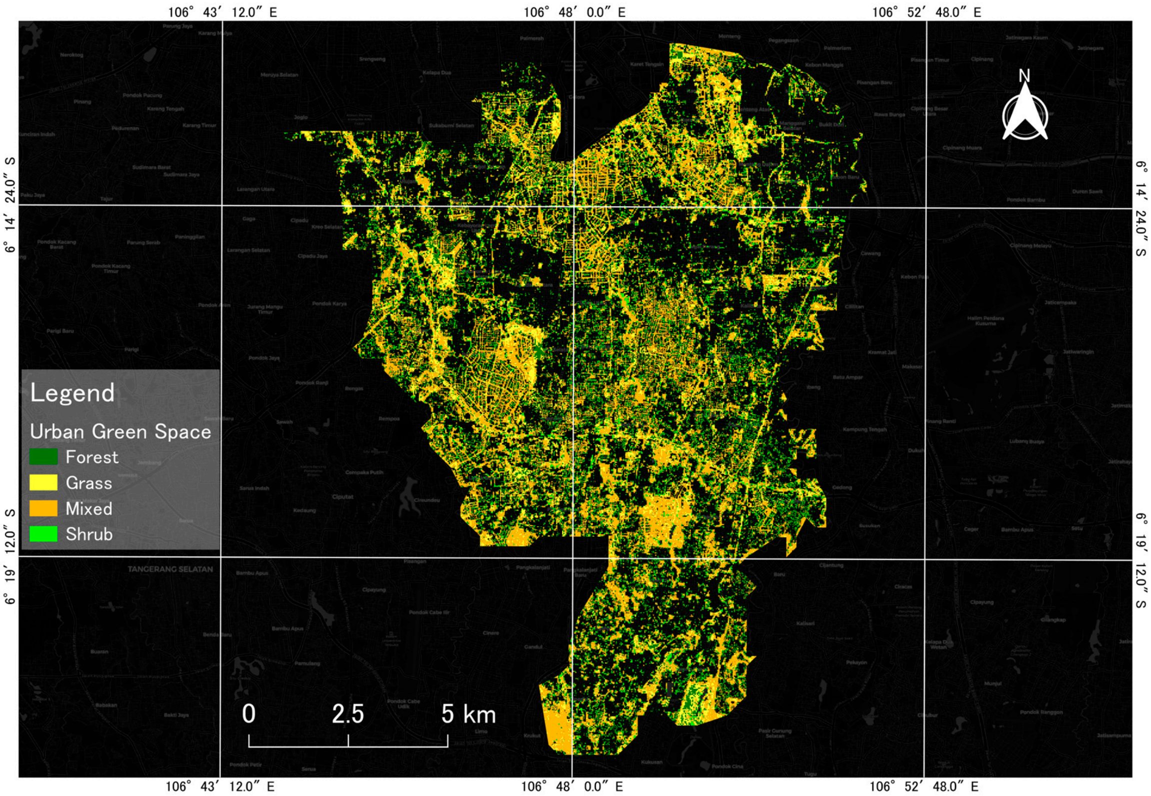

Figure 13. Urban green space of South Jakarta. The base map is CartoDB Dark Matter. QGIS version 3.22.8-Białowieża was used to create the map.

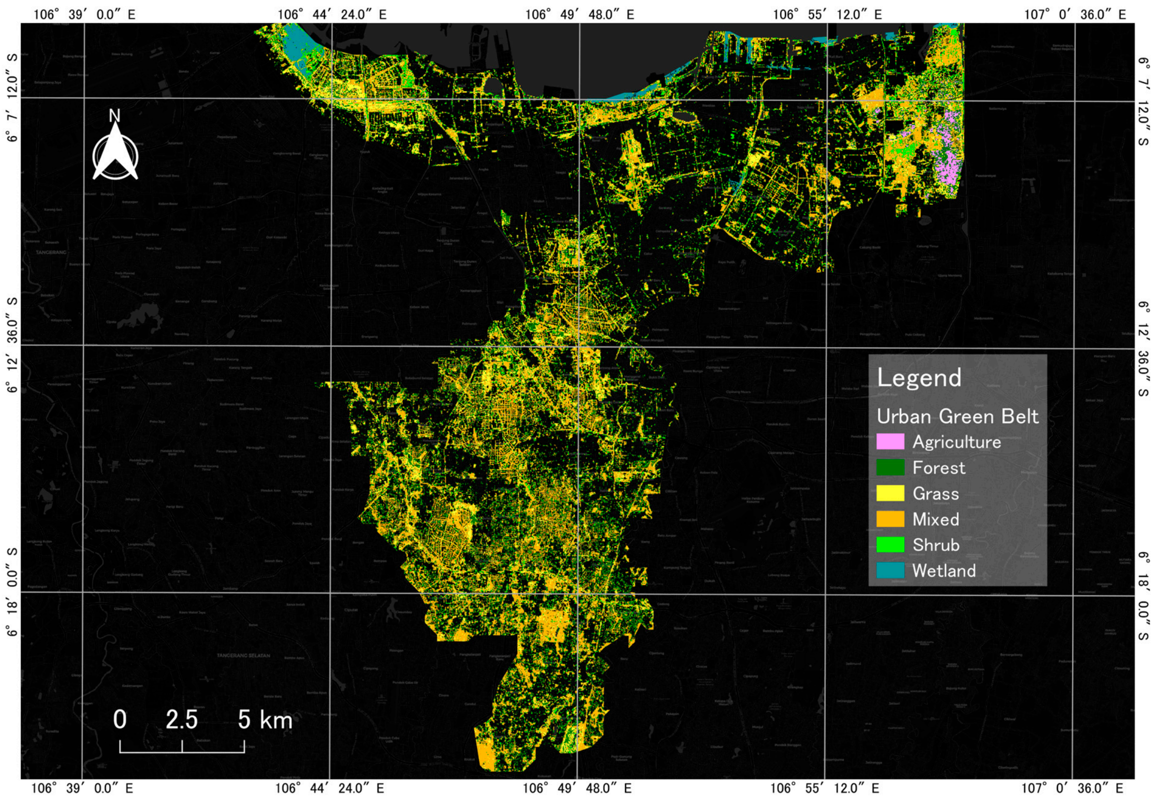

Figure 14. Map of Jakarta's urban green belt. The base map is CartoDB Dark Matter. QGIS version 3.22.8-Białowieża was used to create the map.

Some parts of Jakarta's urban green belt are located in exclusive areas, which means limited access to the public or even closed to the public, such as elite residential green areas and exclusive golf courses. However, a large part is still open to the public such as Ragunan Zoo and City Forest within the University of Indonesia in South Jakarta; the Gelora Bung Karno Complex, Gelora Bung Karno City Forest, and the Monas Complex in Central Jakarta; and Angke Kapok mangrove forest, Kemayoran City Forest, and Penjaringan City Forest Park in North Jakarta.

Jakarta's urban green belt areas are essential components of the city's urban planning and environmental sustainability efforts. These areas play a crucial role in preserving natural ecosystems, enhancing the city's resilience to environmental challenges, and improving the overall quality of life for its residents. Some benefits of these areas are summarized in Table 5.

Table 5. Benefits of Jakarta's urban green belt.

Benefit	Description
Environmental Conservation	Green belt areas in Jakarta are primarily established to conserve natural habitats, including forests and wetlands. These areas are vital for maintaining biodiversity and providing habitats for wildlife.
Flood Mitigation	Jakarta is prone to seasonal flooding, exacerbated by urban expansion. Green belts act as natural buffers, absorbing excess rainwater and reducing the risk of flooding in the city.
Urban Planning and Development Control	Green belt areas serve as a means of regulating urban development. Zoning regulations restrict construction in these zones, ensuring that urban sprawl is controlled and that green spaces are preserved.
Recreational and Educational Opportunities	Many green belt areas in Jakarta are open to the public and offer recreational activities such as walking, biking, or bird watching. These spaces also serve as outdoor classrooms for environmental education.
Economic Benefits	The preservation of green belt areas can have long-term economic benefits, including improved property values in nearby urban areas, increased tourism, and potential for sustainable agriculture or city ecotourism.

However, despite the benefits, Jakarta's urban green belt areas face challenges such as land use conflicts and inadequate enforcement of zoning regulations. These challenges can lead to the degradation of these critical natural spaces. It is suggested that the Jakarta government collaborates with various stakeholders and implements policies and programs aimed at protecting and enhancing green belt areas. This may include reforestation efforts, public awareness campaigns, and stricter land use regulations. Jakarta's green belt areas are likely to become even more critical in the face of climate change and urbanization. Urban green space has an important role to play in creating a culture of health and well-being [33]. However, the availability of urban green space can also increase the land price [34]. Future planning should focus on strengthening conservation efforts, expanding green belts where possible, and integrating them into a broader sustainable urban development strategy.

4. Discussion

4.1. Driving Forces and Comparison of Other Existing Products

The primary driving force behind the creation of large-scale urban green spaces in Jakarta is the governor's policy, particularly Policy No. 9 of 2022 regarding green spaces [35]. This policy aims to ensure that Jakarta allocates 20% of its land to public green spaces and 10% to private green spaces. Activities include enhancing the quantity, quality, and coverage of urban green spaces.

The urban green space master plan involves two crucial steps: strategic policy and an action plan. Within the strategic policy, collaboration between the public and government in managing urban green spaces stands out as pivotal. The government pledges financial, human, and technological resources, along with infrastructure and tools for green space management, research, and technical assistance. Meanwhile, the public is encouraged to establish citizen communities or forums to oversee urban green spaces.

The action plan includes the development of an urban green space database, the revitalization of upstream areas through reforestation and afforestation, and the naturalization of rivers in critical areas. It also entails the restructuring of dense slum settlements along riverbanks, the revitalization of downstream areas through mangrove reforestation, and the monitoring and evaluation of Jakarta's urban green spaces. The implementation of this policy is resulting in an expansion of urban green spaces throughout Jakarta.

However, according to the official data from the Ministry of Environment and Forestry of Indonesia, Jakarta's urban green space is notably scarce, measuring only 3.254 km^2 as of 2023 [36]. This disparity arises from differing definitions of urban green space. The Ministry defines green space as elongated areas or clusters with open usage, where plants naturally grow or are deliberately cultivated [37]. However, this definition is too narrow. In this study, urban green space is defined more precisely and categorized into five classes: agriculture, forest, grassland, mixed, shrub, and wetland. Other research [38] utilizing data from the Department of Human Settlements for Spatial Planning and Land Affairs of DKI Jakarta Province indicates that Jakarta's urban green space measures only 83.55 km^2. This indicates the urban green space of Jakarta is only 12.6%. This underestimated area of urban green space is due to the data sources referring to different years, different publicly editable sources (open street map), and low-resolution Landsat-8 images.

4.2. Advantages

The availability of PlanetScope data through the standard education and research license, along with Sentinel-1 and Sentinel-2 data in the GEE data catalog, opens up diverse possibilities for mapping and monitoring the environment. Specifically, the high resolution of PlanetScope data provides researchers and stakeholders with the means to enhance the level of detail in urban green space analysis in developing countries. In this context, this research seeks to evaluate the potential of PlanetScope data combined with Sentinel-1 and Sentinel-2 data for classifying urban green spaces in Jakarta with great precision and efficiency in terms of computation time.

Prior to conducting the analysis using GEE, attempts were made to process a massive 4.5 GB mosaic of PlanetScope data to classify urban green spaces in Jakarta using QGIS. After waiting for two days, the results proved inadequate, as QGIS encountered an error and became unresponsive. In stark contrast, when utilizing the GEE platform, all that was required was uploading the data to the cloud project. With a user-friendly programming interface and intuitive JavaScript code, the process was completed in a matter of minutes, yielding highly satisfactory results.

4.3. Limitations

Despite its advantages, the proposed methodology has certain limitations. For instance, when utilizing the free version of GEE, one will encounter various constraints, such as storage and image size limitations. To circumvent potential errors in computation time and storage issues, it is necessary to resample all images to a 30 m spatial resolution before proceeding with the classification process. Additionally, it should be borne in mind that a single query to Earth Engine is restricted to a 10 MB size limit. This limit is typically exceeded only when including large additional data directly in the query, like a shapefile or a GeoJSON structure that has been embedded within the query. Another limitation is that free GEE accounts are only permitted to ingest up to 250 GB of space and 10,000 assets.

On the 14 August 2023 acquisition, the PlanetScope data did not provide complete coverage of the study area, with particular limitations in the East Jakarta region, covering approximately 96%. This limitation is primarily attributed to cloud cover issues, which are especially prominent in tropical regions like Indonesia and pose a significant challenge for passive remote sensing.

The PlanetScope data acquired on 14 August 2023 yield the best available dataset for the study area. However, it is worth noting that other datasets exhibit cloud cover exceeding 50%. This resulted in a discrepancy between the total area classification and the administrative boundary. Additionally, not all of North and East Jakarta's urban green spaces were classified. Furthermore, Kepulauan Seribu was excluded from the analysis because it lacks a substantial urban green space, and most of its green space is primarily designated for cemeteries. New artificial islands located in the northern part of Jakarta were also not included in the analysis.

4.4. Future Study

The proposed method for classifying urban green spaces using multiple datasets does not incorporate advanced data fusion techniques; it simply stacks multiple images into single images using the "add.Bands" function within the GEE platform. Hence, it is recommended that future research delves into advanced fusion techniques and assesses their outcomes. Such evaluation should not only prioritize accuracy but also factor in computational efficiency.

5. Conclusions

This study successfully assessed the benefits of employing a supervised classification approach with two different classifier algorithms within the GEE platform. The examination encompassed the PlanetScope-only bands as well as combinations of multiple bands from Sentinel-1 and Sentinel-2, alongside two proposed indexes, RTVI and RTWI.

When using only the PlanetScope bands and the RF classifier algorithm, the accuracy reached 84.9%. However, by incorporating multiple image sources, accuracy significantly improved to 95.9%. The CART classifier algorithm, when applied solely to PlanetScope bands, achieved an accuracy of 85.1%, which saw a slight increase to 87.7% with the inclusion of multiple images. The performance of the RF classifier algorithm demonstrated that all the bands used significantly contributed to the classification.

On average, Jakarta's urban areas cover approximately 33.2% of green spaces. Data and maps from this study can be utilized by urban residents, researchers, and stakeholders interested in urban green spaces. These maps enable the exploration and promotion of a healthier lifestyle, the measurement of landscape metrics, the monitoring of urban green space conditions, and a detailed assessment of existing urban green spaces in Jakarta.

The urban green belt areas in Jakarta play a crucial role in preserving the city's natural heritage, reducing environmental risks, and promoting sustainable urban development. It is important for academic research and policy initiatives to consistently prioritize the protection and improvement of these green spaces. This ensures a healthier and more resilient future for Jakarta and its residents.

Funding: This research was supported by the University of Tsukuba.

Data Availability Statement: Google Earth Engine was utilized via https://code.earthengine.google.com/ (accessed on 12 December 2023) to query Sentinel-1 and Sentinel-2 images and generate spectral indices (RTVI and RTWI) from the PlanetScope images. Preprocessing and classification were executed within the GEE environment. The GEE codes developed in this research are available upon any reasonable request via email. Additionally, various other tasks were completed, including converting images into polygons, correcting geometries, adding new fields, dissolving features, and calculating areas, all conducted using QGIS 3.22.8-Białowieża. The data resulting from this study on Jakarta's urban green space, with very high spatial resolution and high accuracy, are publicly available on Zenodo: https://doi.org/10.5281/zenodo.10472507.

Conflicts of Interest: The author declares no conflict of interest.

References

1. Groenewegen, P.P.; Van Den Berg, A.E.; De Vries, S.; Verheij, R.A. Vitamin G: Effects of green space on health, well-being, and social safety. *BMC Public Health* **2006**, *6*, 149. [CrossRef] [PubMed]
2. Jabbar, M.; Yusoff, M.M.; Shafie, A. Assessing the role of urban green spaces for human well-being: A systematic review. *GeoJournal* **2022**, *87*, 4405–4423. [CrossRef] [PubMed]
3. Yang, H.; Chen, T.; Zeng, Z.; Mi, F. Does urban green space justly improve public health and well-being? A case study of Tianjin, a megacity in China. *J. Clean. Prod.* **2022**, *380*, 134920. [CrossRef]
4. Nasrabadi, M.T.; Morassafar, S.; Pourzakarya, M.; Dunning, R. Investigating the impacts of green spaces planning on social sustainability improvement in Tehran, Iran: A SWOT-AHP analysis. *Local Environ.* **2023**, *28*, 681–697. [CrossRef]
5. Madureira, H.; Nunes, F.; Oliveira, J.V.; Cormier, L.; Madureira, T. Urban residents' beliefs concerning green space benefits in four cities in France and Portugal. *Urban For. Urban Green.* **2015**, *14*, 56–64. [CrossRef]
6. Jansson, M. Green space in compact cities: The benefits and values of urban ecosystem services in planning. *Nord. J. Archit. Res.* **2014**, *26*, 139–160.
7. Enssle, F.; Kabisch, N. Urban green spaces for the social interaction, health and well-being of older people—An integrated view of urban ecosystem services and socio-environmental justice. *Environ. Sci. Policy* **2020**, *109*, 36–44. [CrossRef]
8. Xu, T.; Nordin, N.A.; Aini, A.M. Urban Green Space and Subjective Well-Being of Older People: A Systematic Literature Review. *Int. J. Environ. Res. Public Health* **2022**, *19*, 14227. [CrossRef]
9. White, M.P.; Elliott, L.R.; Grellier, J.; Economou, T.; Bell, S.; Bratman, G.N.; Cirach, M.; Gascon, M.; Lima, M.L.; Lõhmus, M.; et al. Associations between green/blue spaces and mental health across 18 countries. *Sci. Rep.* **2021**, *11*, 8903. [CrossRef]
10. Wortzel, J.D.; Wiebe, D.J.; DiDomenico, G.E.; Visoki, E.; South, E.; Tam, V.; Greenberg, D.M.; Brown, L.A.; Gur, R.C.; Gur, R.E.; et al. Association Between Urban Greenspace and Mental Wellbeing During the COVID-19 Pandemic in a U.S. Cohort. *Front. Sustain. Cities* **2021**, *3*, 686159. [CrossRef]
11. Sathyakumar, V.; Ramsankaran, R.; Bardhan, R. Linking remotely sensed Urban Green Space (UGS) distribution patterns and Socio-Economic Status (SES)—A multi-scale probabilistic analysis based in Mumbai, India. *GISci. Remote Sens.* **2019**, *56*, 645–669. [CrossRef]
12. Ramdani, F. Urban Vegetation Mapping from Fused Hyperspectral Image and LiDAR Data with Application to Monitor Urban Tree Heights. *J. Geogr. Inf. Syst.* **2013**, *2013*, 404–408. [CrossRef]
13. Shi, Q.; Liu, M.; Marinoni, A.; Liu, X. UGS-1m: Fine-grained urban green space mapping of 31 major cities in China based on the deep learning framework. *Earth Syst. Sci. Data* **2023**, *15*, 555–577. [CrossRef]
14. Huang, Y.; Lin, T.; Zhang, G.; Zhu, Y.; Zeng, Z.; Ye, H. Spatial patterns of urban green space and its actual utilization status in China based on big data analysis. *Big Earth Data* **2021**, *5*, 391–409. [CrossRef]
15. Zhu, Z.; Li, J.; Chen, Z. Green space equity: Spatial distribution of urban green spaces and correlation with urbanization in Xiamen, China. *Environ. Dev. Sustain.* **2023**, *25*, 423–443. [CrossRef]
16. Ju, Y.; Dronova, I.; Delclòs-Alió, X. A 10 m resolution urban green space map for major Latin American cities from Sentinel-2 remote sensing images and OpenStreetMap. *Sci. Data* **2022**, *9*, 586. [CrossRef] [PubMed]
17. Tassi, A.; Vizzari, M. Object-Oriented LULC Classification in Google Earth Engine Combining SNIC, GLCM, and Machine Learning Algorithms. *Remote Sens.* **2020**, *12*, 3776. [CrossRef]
18. Vizzari, M. PlanetScope, Sentinel-2, and Sentinel-1 Data Integration for Object-Based Land Cover Classification in Google Earth Engine. *Remote Sens.* **2022**, *14*, 2628. [CrossRef]
19. BPS. Jumlah Penduduk Menurut Kabupaten/Kota di Provinsi DKI Jakarta. *Badan Pusat Statistik.* 2022. Available online: https://jakarta.bps.go.id/indicator/12/1270/1/jumlah-penduduk-menurut-kabupaten-kota-di-provinsi-dki-jakarta-.html (accessed on 15 January 2024).
20. BPS. Luas Daerah Menurut Kabupaten/Kota. *Badan Pusat Statistik.* 2022. Available online: https://jakarta.bps.go.id/indicator/153/38/1/luas-daerah-menurut-kabupaten-kota.html (accessed on 15 January 2024).
21. Demographia. Demographia World Urban Areas (19th Annual Edition). *Demographia.* 2023. Available online: http://www.demographia.com/db-worldua.pdf (accessed on 20 January 2024).
22. Planet. Planet Imagery Product Specifications. *Planet Lab PBC.* 2022. Available online: https://assets.planet.com/docs/Planet_Combined_Imagery_Product_Specs_letter_screen.pdf (accessed on 20 January 2024).
23. Planet. Beyond NDVI with Planetscope 8-Band Data. *Planet.* 2022. Available online: https://learn.planet.com/rs/997-CHH-265/images/Beyond%20NDVI%20Datasheet.pdf (accessed on 20 January 2024).
24. ESA. Sentinel-1. *The European Space Agency.* 2022. Available online: https://sentinels.copernicus.eu/web/sentinel/missions/sentinel-1 (accessed on 25 January 2024).
25. ESA. Sentinel-2. *The European Space Agency.* 2022. Available online: https://sentinels.copernicus.eu/web/sentinel/missions/sentinel-2 (accessed on 25 January 2024).
26. Gislason, P.O.; Benediktsson, J.A.; Sveinsson, J.R. Random forests for land cover classification. *Pattern Recognit. Lett.* **2006**, *27*, 294–300. [CrossRef]
27. Pal, M. Random forest classifier for remote sensing classification. *Int. J. Remote Sens.* **2005**, *26*, 217–222. [CrossRef]
28. Belgiu, M.; Drăguţ, L. Random forest in remote sensing: A review of applications and future directions. *ISPRS J. Photogramm. Remote Sens.* **2016**, *114*, 24–31. [CrossRef]

29. Friedl, M.A.; McIver, D.K.; Hodges, J.C.F.; Zhang, X.Y.; Muchoney, D.; Strahler, A.H.; Woodcock, C.E.; Gopal, S.; Schneider, A.; Cooper, A.; et al. Global land cover mapping from MODIS: Algorithms and early results. *Remote Sens. Environ.* **2002**, *83*, 287–302. [CrossRef]
30. Lawrence, R.L.; Wright, A. Rule-based classification systems using classification and regression tree (CART) analysis. *Am. Soc. Photogramm. Remote Sens.* **2001**, *67*, 1137–1142.
31. Shao, Y.; Lunetta, R.S. Comparison of support vector machine, neural network, and CART algorithms for the land-cover classification using limited training data points. *ISPRS J. Photogramm. Remote Sens.* **2012**, *70*, 78–87. [CrossRef]
32. FAO. Global Administrative Unit Layers (GAUL). *Food and Agricultutral Organization of the United Nations.* 2015. Available online: https://data.apps.fao.org/map/catalog/srv/eng/catalog.search?id=12691#/metadata/9c35ba10-5649-41c8-bdfc-eb78e9e65654 (accessed on 9 September 2023).
33. Hunter, R.F.; Cleary, A.; Braubach, M. Environmental, Health and Equity Effects of Urban Green Space Interventions. In *Biodiversity and Health in the Face of Climate Change*; Springer: Berlin/Heidelberg, Germany, 2019. [CrossRef]
34. Wolch, J.R.; Byrne, J.; Newell, J.P. Urban green space, public health, and environmental justice: The challenge of making cities 'just green enough'. *Landsc. Urban Plan.* **2014**, *125*, 234–244. [CrossRef]
35. Governor of DKI Jakarta. Peraturan Gubernur Daerah Khusus Ibukota Jakarta Nomor 9 Tahun 2022 Tentang Ruang Terbuka Hijau. 2022. Available online: https://jdih.jakarta.go.id/dokumenPeraturanDirectory/0031/202225009.pdf (accessed on 8 April 2024).
36. MOEF. Ruang Terbuka Hijau. 2023. Available online: https://sipsn.menlhk.go.id/sipsn/public/rth (accessed on 8 April 2024).
37. MOEF. Peraturan Menteri Kehutanan Republik Indonesia Nomor: P.71/Menhut-Ii/2009 Tentang Pedoman Penyelenggaraan Hutan Kota. 2009. Available online: https://jdih.menlhk.go.id/new/uploads/files/P.71%20(4).pdf (accessed on 8 April 2024).
38. Hwang, Y.H.; Nasution, I.K.; Amonkar, D.; Hahs, A. Urban Green Space Distribution Related to Land Values in Fast-Growing Megacities, Mumbai and Jakarta–Unexploited Opportunities to Increase Access to Greenery for the Poor. *Sustainability* **2020**, *12*, 12. [CrossRef]